Protolytic Reactions on Reduction of Cytochrome *c* Oxidase Studied by ATR-FTIR Spectroscopy†

Elena A. Gorbikova,* Nikolai P. Belevich, Mårten Wikström, and Michael I. Verkhovsky

Program for Structural Biology and Biophysics, Institute of Biotechnology, PB 65 (Viikinkaari 1), University of Helsinki, Helsinki FIN-00014, Finland

Received December 7, 2006; Revised Manuscript Received January 30, 2007

ABSTRACT: Reduction of cytochrome *c* oxidase is coupled to proton uptake, and the reduced-minus-oxidized FTIR spectrum should include signatures of protonation of protolytic centers. The major part of the spectrum shows only small differences between acidic and alkaline conditions, which is consistent with the rather weak pH dependence of the proton uptake stoichiometry. Here we aim at revealing redox state-dependent protonatable sites and present a comprehensive investigation over a wide pH range. The reduced-minus-oxidized transition of cytochrome *c* oxidase from *Paracoccus denitrificans* was studied by means of Fourier transform infrared spectroscopy in the pH range 5.2−9.5. Effects of pH were analyzed as the difference between reduced-minus-oxidized FTIR spectra at different pH values. Two pH-dependent processes with apparent pK_a values of 6.6 and 8.4 and Hill coefficients 0.9 and 0.1, respectively, were found by this methodology. A sharp OH band appears in the IR "water region" on reduction of the enzyme, independent of pH in the range 6.5−9.0, and downshifted by ∼940 cm^{-1} on changing the solvent to D_2O and by 10 cm^{-1} on $H_2{}^{16}O/H_2{}^{18}O$ isotope exchange. This feature of an asymmetric water molecule may belong to water that is produced in the binuclear center upon reduction or to a structured water molecule that loses a hydrogen bond.

Cytochrome *c* oxidase (C*c*O)[1] or complex IV is the terminal enzyme of the respiratory chain of mitochondria and many aerobic bacteria. C*c*O functions as a redox-driven proton pump and generates a transmembrane difference of electrochemical potential of protons which is used for the synthesis of ATP (for reviews see refs *1*−*3*).

Cu_A, heme *a*, heme a_3, and Cu_B are the redox centers in aa_3-type cytochrome *c* oxidases. The natural electron donor is cytochrome *c*, a water-soluble electron carrier that circulates between ubiquinol:cytochrome *c* oxidoreductase (complex III) and cytochrome *c* oxidase. Cytochrome *c* passes electrons to Cu_A; then they are transferred further to heme *a* and finally to a binuclear reaction center composed of heme a_3 and Cu_B. During four-electron reduction of oxygen to water (which takes place in the binuclear center), four protons ("pumped" protons) are actively translocated across the membrane. Four more protons ("chemical" protons) are transferred from the negatively charged N-side of the membrane to the binuclear center where they are consumed during the reduction of oxygen to water. The catalytic mechanism of C*c*O is complicated, and some relatively stable states have been resolved (*1*, *4*−*6*). The paths of electron and proton transfer have been deduced from the transient kinetics of membrane potential formation and from optical measurements (*7*−*10*). However, neither these studies, nor the structures of C*c*O (*11*−*14*), have revealed the protonation/deprotonation events of chemical groups responsible for proton transfer, except indirectly (*15*). One of the most promising methods that may allow such information is Fourier transform infrared (FTIR) spectroscopy (*16*) that has perhaps most successfully been applied on proton transfer in bacteriorhodopsin (see, for example, refs *17* and *18*). The ATR-FTIR technique has been applied to several enzymes (*19*−*22*), including studies of redox-induced changes (*21*−*23*). ATR-FTIR spectroscopy operates on an immobilized protein film with a working thickness of around 2 μm in the middle infrared range.

Protolytic reactions of cytochrome *c* oxidase were extensively studied by the groups of Rich and Hellwig using red-minus-ox FTIR spectra in the 2000−1000 cm^{-1} region (see, for example, refs *24* and *25* and refs *26* and *27*, respectively). Such spectra at acidic and alkaline pH have shown only small differences (*28*, *29*), which is consistent with the general finding that the stoichiometry of proton uptake on C*c*O reduction in *Paracoccus denitrificans* is weakly pH-dependent (*30*; unpublished data on the *P. denitrificans* enzyme in the pH region 6−10).

In this work we have performed extensive pH titrations of the red-minus-ox FTIR spectrum of aa_3 oxidase from *P. denitrificans* in the pH range 5.2−9.5 and analyzed its pH dependence. We have further extended the red-minus-ox spectra into the infrared "water region" where we observed

† This work was supported by the Academy of Finland (project numbers 200726 and 44895), Biocentrum Helsinki, and the Sigrid Jusélius Foundation. E.A.G. was supported by The ISB Graduate School.

* To whom correspondence should be addressed. Phone: +358 9 191 59922. Fax: +358 9 191 59920. E-mail: elena.gorbikova@helsinki.fi.

[1] Abbreviations: ATR, attenuated total reflectance; CE, counter electrode; C*c*O, cytochrome *c* oxidase; ΔOD, difference in optical density; E_m, midpoint redox potential (relative to NHE); FTIR, Fourier transform infrared; IR, infrared; red, reduced; NHE, normal hydrogen electrode; N-side, negatively charged side of membrane; ox, oxidized; redox, oxidoreduction; RE, reference electrode; WE, working electrode.

10.1021/bi602523a CCC: $37.00
Published on Web 03/07/2007

two sharp IR modes on reduction of the enzyme; one of them is sensitive to H/D isotope exchange and the other to both H/D and $H_2{}^{16}O/H_2{}^{18}O$ exchange.

MATERIALS AND METHODS

Sample Preparation. An "ATR-ready" sample of cytochrome *c* oxidase from *P. denitrificans* was prepared and deposited on the ATR prism essentially as described in ref *21*)with modifications (*29*, *31*). The differences in handling with the ATR-ready sample were the following. The signal intensity of the amide I band of the dried film was 1.2−1.3. Then, the protein film was rewetted with 40 μL of titration buffer and left in such conditions for 30−40 min. The signal intensity of the amide I band of the rewetted film was 1.1 in all samples, which confirms that the concentration of protein in the beam path was the same. After the rewetting and a 30−40 min delay, the sample was covered with the chamber that allowed a continuous flow of buffer over the sample surface, driven by a peristaltic pump at a flow rate of 2 mL/min. The protein film was stabilized overnight with continuous pumping.

Electrochemistry. To set the redox potential, a homemade flow-through electrochemical cell (*32*) was used. Gold grains (diameter 0.3−0.5 mm) were used as the working electrode (WE), a platinum-plated titanium grid as the counter electrode (CE), and Ag/AgCl/saturated KCl as the reference electrode (RE). Essential details of the cell with application to cytochrome *c* oxidase oxidoreduction were described in ref *29*. The middle compartment of the cell was filled with the titration buffer (400 mM K_2SO_4, 25 mM potassium acetate, 25 mM potassium phosphate, and 25 mM boric acid).

The electrochemical cell was connected to a Princeton Applied Research potentiostat, and the potential was set automatically by the software. To reduce the enzyme, the potential was set at −300 mV vs NHE; to oxidize, at +480 mV.

To equilibrate the enzyme film with the potential of the working electrode, two mediators were used: 1,2-diaminocyclohexane-*N*,*N*,*N*′,*N*′-tetraacetic acid + Fe, E_m +95 mV, and ferrocene acetate, E_m +370 mV. Each mediator was used at a concentration of 200 μM. Due to the low stability of ferrocene acetate at high potentials during the experiment (ca. 15 h), the same amount was added gradually to the buffer along the titration.

The kinetics of the equilibration process was controlled spectrophotometrically at 445 nm. The selected mediators did not show any significant contribution to the infrared or visible spectral regions as compared to the enzyme absorption.

pH Titration. pH titrations were performed in the pH range 5.2−9.5 in an automatic mode in both directions. First, the background (BG) in the infrared (IR) region was measured at the reducing potential. Then the potential was switched to the oxidative one. After 25 min of equilibration, the sample spectrum in the infrared region was measured to generate an ox-minus-red FTIR spectrum. Immediately after this, a new BG was taken in the IR, and then the potential was switched to the reductive one. Again, after 25 min of equilibration, a new spectrum in the IR region was measured to generate the red-minus-ox FTIR spectrum. After that, an aliquot of KOH (5 M), or H_2SO_4 (1 M), was automatically injected by the syringe pump into the titration buffer (400 mM K_2SO_4, 25 mM potassium acetate, 25 mM potassium phosphate, and 25 mM boric acid). After a delay of 25 min for pH equilibration in the whole titration system (electrochemical cell and reservoir, 50 mL overall), the described procedure was repeated.

High ionic strength (400 mM K_2SO_4) jointly with a relatively low buffer capacity (25 mM potassium acetate, 25 mM potassium phosphate, and 25 mM boric acid) allowed minimization of protein changes that could be caused by ionic strength alterations on titrant (KOH or H_2SO_4) addition.

Spectroscopy. A Bruker IFS 66s FTIR spectrometer (equipped with an MCT detector) and a USB2000 visible spectrophotometer (Ocean Optics) were used. FTIR spectra were measured in the range 4000−500 cm^{-1} with 4 cm^{-1} spectral resolution, scanner frequency 80 kHz, apodization function Blackman−Harris 3-term. The number of scans in background and sample spectra was 1024 or 2000. The light guide of the visible spectrophotometer was connected to the ATR cell, which allowed simultaneous collection of FTIR spectra and equilibration kinetics in the visible range. All measurements were performed at room temperature.

The whole titration process (initializing, sending commands to/from Ocean Optics and FTIR Opus software, and collecting data) was controlled by Titrator software designed in our laboratory by N. Belevich.

H/D Exchange. H/D isotope exchange of *P. denitrificans* aa_3 oxidase was performed directly on the ATR prism. The dried enzyme film was rewetted with D_2O (pD 9.0) followed by at least 18 h of isotope exchange. The amplitude of the amide I band of the D_2O rewetted film was 0.9. The level of H/D exchange of amide groups was estimated as described in ref *33* to ∼50%.

Measurements of redox transitions in D_2O were carried out in another electrochemical cell that was designed and first applied in ref *22*. The advantage of this cell for D_2O measurements is a small working volume of ca. 20 μL. Methyl viologen, E_m −446 mV, and ferricyanide, E_m +440 mV, were used as mediators at a concentration of 200 μM each. The potential was switched between −420 and +550 mV. The buffer composition was the same as in the pH-titration experiments, except that D_2O was used instead of H_2O. Because of the absence of visible optics in this electrochemical cell, equilibration was controlled by the amplitude of differential FTIR spectra and took 30−60 min. A total of 4000−8000 scans were averaged for each pH(D) value (6.5 and 9.0) to produce the final red-minus-ox spectra.

$H_2{}^{16}O/H_2{}^{18}O$ Isotope Exchange. The $H_2{}^{16}O/H_2{}^{18}O$ isotope exchange was done directly on enzyme positioned on the ATR prism. $H_2{}^{18}O$ (Cambridge Isotopes) contains 95% ^{18}O. The $H_2{}^{18}O$ concentration in the final buffer was 85%, which is expected to result in an $^{16}OH \rightarrow {}^{18}OH$ band shift of 14 cm^{-1} (*45*). To perform the $H_2{}^{18}O$ measurements, the 20 μL electrochemical cell described in the previous section was used. Buffer composition was the same as in all experiments described above; pH 6.5. 1,2-Diaminocyclohexane-*N*,*N*,*N*′,*N*′-tetraacetic acid + Fe, E_m +95 mV, and ferricyanide, E_m +440 mV, were used as redox mediators at a concentration of 500 μM each. The junction between the enzyme compartment and the RE was filled with the same buffer to decrease $H_2{}^{16}O$ leakage from the RE. The reductive and oxidative potentials were −300 and +550 mV, respectively. The low

reductive potential was set to reduce oxygen that possibly leaks into the enzyme compartment. The equilibration process was controlled by following the amplitude of the redox signal and took less than 15 min. To get the final spectrum, red-minus-ox and ox-minus-red data were averaged. The final number of interferograms was 49152 (48 spectra × 1024 scans each).

Data Analysis. Every ox-minus-red FTIR difference spectrum was averaged with the corresponding red-minus-ox spectrum. All red-minus-ox FTIR spectra were normalized to each other by the 1661/1641 cm^{-1} peak difference. All red-minus-ox spectra in the whole pH region were subtracted from the most acidic or alkaline one. Baseline correction of amide bands was done at pH values below 7 and higher than 8. pH-titration surfaces (dependence of ΔOD on pH and wavenumber) were generated. Titration curves (dependence of ΔOD on the applied pH at peaks and troughs) were extracted from the "pH surfaces" in the 1800−1200 cm^{-1} region. The intensity of every peak was defined as the difference between the intensity at the peak (trough) and half the sum of the intensities of the adjacent troughs (peaks). The intensity of every shift was estimated as the difference between the intensity at the peak (trough) and the intensity at the adjacent troughs (peak). All calculation and fitting procedures were performed in Matlab software.

RESULTS

Electrochemically Induced Red-minus-Ox FTIR Spectra at Acidic and Alkaline pH. The pH dependence of the difference between the reduced and oxidized states of cytochrome *c* oxidase was measured by means of a combination of electrochemical and FTIR spectroscopic approaches. The potentials set by the potentiostat corresponded to −300 and +480 mV for the reduced and oxidized states, respectively. Red-minus-ox spectra were measured in the pH range 5.2−9.5 with steps of 0.2−0.7 pH unit. At each pH step, FTIR spectra were collected in both directions: red-minus-ox and ox-minus-red. For further analysis, spectra in both directions were averaged at each pH step. All spectra were normalized to each other by the peak difference at 1661/1641 cm^{-1}. Red-minus-ox FTIR difference spectra at pH 5.2 and 9.5 are shown in Figure 1 and are similar to those published earlier (*28*). They reveal relatively small changes in the amide I (1700−1600 cm^{-1}) and II (1600−1500 cm^{-1}) regions, as well as in the 1500−1200 cm^{-1} region in acidic (solid line) and alkaline (dashed line) conditions, which can now be titrated as a function of pH.

It is noteworthy here that there are no significant changes in the 1740 cm^{-1} region ascribed to the well-conserved glutamic acid 278 (242 in bovine and 286 in *Rhodobacter sphaeroides* numbering) in the proton-transferring D-pathway (*34*, *35*).

Acidic-minus-Alkaline Red-minus-Ox Double Difference Spectra. As a result of the pH titration, we obtained red-minus-ox spectra in the pH range 5.2−9.5. All spectra were subtracted from the most acidic or alkaline spectrum to produce double-difference acidic-minus-alkaline or alkaline-minus-acidic red-minus-ox spectra. "ΔOD-pH-wavenumber" surfaces were generated from the double-difference spectra. The development of the individual infrared features in acidic-minus-alkaline red-minus-ox FTIR spectra along the pH titration is shown in Figure 2.

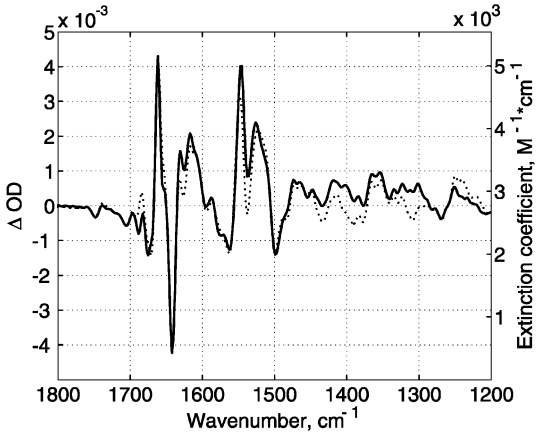

FIGURE 1: Red-minus-ox FTIR spectra of *P. denitrificans* cytochrome *c* oxidase at pH 5.2 (solid line) and 9.5 (dashed line). Typical spectra are shown at the acidic and alkaline marginal points of the pH-titration set. The applied potential step was −300 to +480 mV. Initial red-minus-ox spectra are normalized by the peaks at 1661/1641 cm^{-1}. Estimated extinction coefficients in all figures are the mean values for mid-IR regarding the penetration depth as 2 μm.

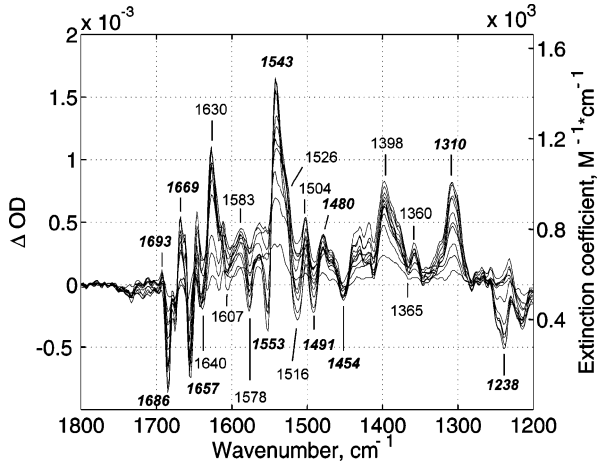

FIGURE 2: Development of the acidic-minus-alkaline red-minus-ox FTIR spectrum. The set of acidic-minus-alkaline red-minus-ox FTIR spectra is produced as a difference between the most acidic red-minus-ox spectrum (pH 5.2) and all other spectra in the alkaline direction. Bands that showed one-component behavior are marked in lightface roman type; bands with two-component behavior are marked in bold italic type (for one- and two-component behavior, see Patterns of pH-Titration Curves in the Results section).

To check the reversibility of the pH effect and to distinguish it from ionic strength changes, the pH titration was performed in two directions: from acidic to alkaline conditions and back. A comparison of acidic-minus-alkaline (from KOH titration, solid line) and alkaline-minus-acidic (from H_2SO_4 titration, dashed line) red-minus-ox spectra is shown in Figure 3. All pH-induced changes are reversible, therefore excluding ionic strength effects.

Patterns of pH-Titration Curves. pH-titration curves of each band and band shift were extracted from the ΔOD-pH-wavenumber surfaces. The whole system of pH-titration curves was unified so that the direction of development of the amplitudes was the same. Data from three sets were analyzed: two sets of KOH titration and one set of H_2SO_4 titration. The titration curves from each of the three sets were divided into two groups according to their pH dependence. The experimental points of all curves from each group were

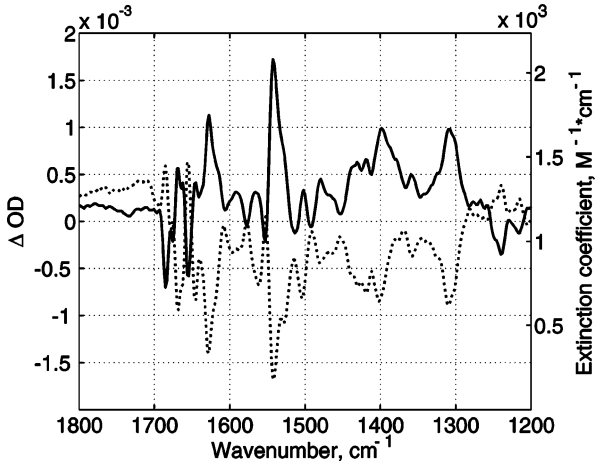

FIGURE 3: Double-difference acidic-minus-alkaline (pH 5.2-minus-pH 9.5, solid line) and alkaline-minus-acidic (pH 9.5-minus-pH 5.2, dashed line) red-minus-ox FTIR spectra. The spectra are from two sets with different directions of pH titration.

averaged within each set and fitted with Henderson−Hasselbalch equations with a variable Hill coefficient. The averaged experimental points of the first group are plotted in Figure 4A (circles). The fit of the first group by a one-component Henderson−Hasselbalch equation resulted in pK_a = 6.6 and Hill coefficient = 0.9 (curve). The averaged experimental points of the second group are shown in Figure 4B (circles). To fit this group, a two-component Henderson−Hasselbalch equation was used (curve) with fixed pK_a and the Hill coefficient taken from the first group. This fit resulted in pK_a and Hill coefficient of the second transition of 8.4 and 0.1. The standard deviations were estimated for each pH point within each of the three titration sets. The IR features that showed one- and two-component pH behavior, respectively, are indicated in Figure 2.

H/D Exchangeable Protons in the Redox Transition. To distinguish direct protonation effects from induced pH effects on the protein and the redox cofactors, we applied H/D isotope exchange. The red-minus-ox spectrum at pD 9.0 (not shown) has the same features in the fingerprint region as those published earlier (*24*, *25*). The main changes of deuterium isotope exchange on acidic-minus-alkaline red-minus-ox FTIR spectra in the 1800−1200 cm^{-1} range are the disappearance of the peak at 1480 cm^{-1} and the trough at 1238 cm^{-1} (Figure 2) and the appearance of a new peak at 1460 cm^{-1} in D_2O (spectra in D_2O are not shown). No clear signatures of H/D isotope shifts of protolytic amino acids in acidic-minus-alkaline (pH 6.5-minus-9.0) red-minus-ox FTIR spectra were found.

We extended our analysis of red-minus-ox FTIR spectra to the water region between 3800 and 2400 cm^{-1} (Figure 5). Two sharp peaks at 3610 and 3566 cm^{-1} and one smaller peak at 3672 cm^{-1} in H_2O medium were absent in D_2O, where several new features appeared: peaks at 2716, 2673, 2639, and 2473 cm^{-1} and two troughs, 2548 and 2515 cm^{-1}. Furthermore, the intensities of bands in the 3000−2800 cm^{-1} region (C−H stretching vibrations of CH_2 and CH_3 groups) were decreased after isotope exchange. It is important to note that the spectra had no pH(D)-dependent differences except the shift at 3348/3324 cm^{-1} and peak at 2962 cm^{-1} that are slightly more intensive at pH(D) 6.5 than at pH(D) 9.0.

$H_2{}^{16}O/H_2{}^{18}O$ Isotope Exchange. From H/D exchange it seems that the bands at 3610 and 3566 cm^{-1} move to 2673 and 2639 cm^{-1}, respectively, which is an ∼940 cm^{-1} shift that corresponds well to OH → OD exchange. To check if the peaks at 3610 and 3566 cm^{-1} belong to water molecules, red-minus-ox FTIR spectra were measured in $H_2{}^{18}O$ medium. The peak at 3610 cm^{-1} was shifted to 3600 cm^{-1} after $H_2{}^{16}O$/$H_2{}^{18}O$ exchange, but the band 3566 cm^{-1} was not significantly affected. The 10 cm^{-1} shift of the 3610 cm^{-1} band upon $H_2{}^{16}O/H_2{}^{18}O$ exchange together with the ∼940 cm^{-1} shift upon H/D exchange helps to assign this to an OH stretching vibration of a water molecule. The oxygen isotope shift of 10 cm^{-1} is a little less than what is expected theoretically (14 cm^{-1}), probably because of diffusion of residual $H_2{}^{16}O$ from the reference electrode and dilution of $H_2{}^{18}O$ buffer.

DISCUSSION

Nature of the pH Effect in Red-minus-Ox FTIR Spectra. Anaerobic redox titrations of cytochrome *c* oxidase from *P. denitrificans* showed uptake of two protons on reduction as judged from the pH dependence of the E_m values: 30 mV/pH unit each of hemes *a* and a_3 and ∼60 mV/pH for Cu_B at alkaline pH (*29*). Mitchell and Rich (*36*) measured proton uptake on reduction of bovine C*c*O and reported ∼2.4 H^+ at neutral pH, two protons being ascribed to linkage to reduction of the binuclear site. Consequently, a fractional proton (0.4 H^+) may be associated with additional reduction of heme *a* and Cu_A. No significant pH dependence of this proton uptake was observed between pH 7.2 and pH 8.5 (*36*). In contrast, Capitanio et al. (*37*) reported a significant pH dependence of the number of H^+ consumed on enzyme reduction.

Protolytic reactions on reduction of cytochrome oxidase may be ascribed to three possible kinds of events: (i) uptake of chemical protons, (ii) protonation and deprotonation of residues involved in the proton-pumping reaction, and (iii) uptake of additional protons, the role of which may be to balance subtle changes in conformation of the redox centers and/or the protein structure on reduction.

It is important to point out that the pH dependence of the acidic-minus-alkaline red-minus-ox FTIR spectra within the tested pH regime would reveal protons in category i *only* if the pK_a values of the chemical proton acceptors were within or close to that regime (see ref *37*). The data of Mitchell and Rich (*36*) suggest that this is not the case, whereas the data of Capitanio et al. (*37*) suggest that it is. The same requirement holds for detection of protonation and deprotonation of residues involved in proton pumping by this methodology (case ii). We note that deprotonation of glutamic acid 278, a key element of proton transfer in the D-pathway, is known to decrease the E_m of heme *a* (*38*, *39*). Such coupling between the redox state of heme *a* and the protonation state of the glutamate implies that reduction of heme *a* should increase the pK_a of E-278. On this basis the red-minus-ox spectrum should include the distinct IR feature of the acid form of E-278 near 1740 cm^{-1} (see above) if the pK_a values were to fall within the pH range studied (5.2−9.5). A functional pK_a value of 9.4 for E-278 has been deduced from kinetic experiments (*40*), implying about half-deprotonation at the highest pH of our experiments. Since this was not observed, we conclude that the equilibrium pK_a of glutamic acid 278 in the oxidized enzyme must be

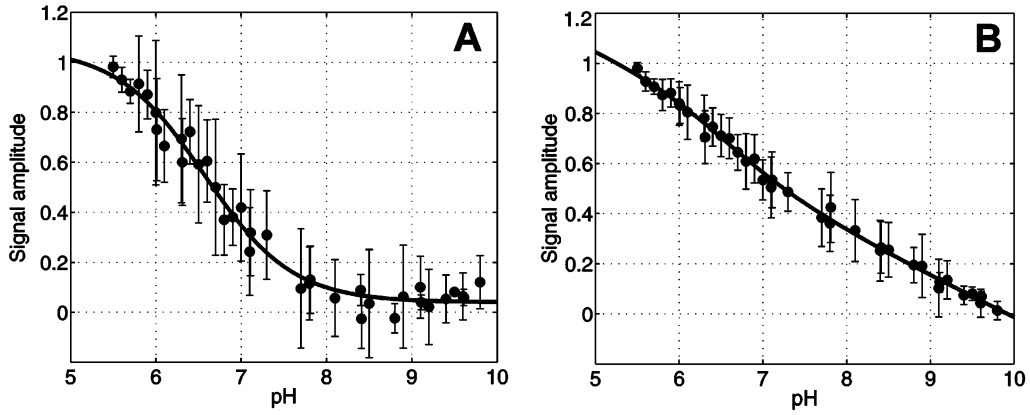

FIGURE 4: Two patterns of pH-titration curves. (A) Group 1, one-component Henderson−Hasselbalch equation, pK = 6.6 and n = 0.9, and (B) group 2, two-component Henderson−Hasselbalch equation, pK_1 = 6.6 and n = 0.9 were obtained from group 1 and fixed, and pK_2 = 8.4 and n = 0.1. Experimental points of three sets are normalized by maximal amplitude and plotted together with theoretical curves. Averages of data points within each of three sets are shown together with the standard deviations.

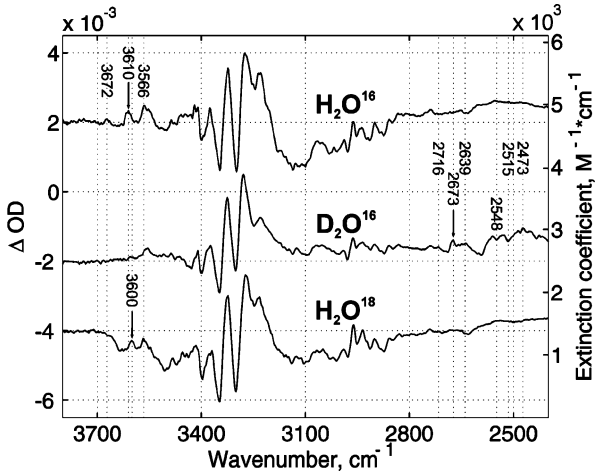

FIGURE 5: Isotope H/D and $H_2{}^{16}O/H_2{}^{18}O$ effect on red-minus-ox FTIR spectra of *P. denitrificans* C*c*O in the water region. The upper spectrum is an average of the spectra at pH 6.5 and 9.0 in $H_2{}^{16}O$ medium, the middle spectrum is an average of spectra at pD 6.5 and 9.0 in $D_2{}^{16}O$ medium, and the lower spectrum is at pH 6.5 in $H_2{}^{18}O$ medium. All spectra were normalized in the fingerprint region by the 1661/1641 cm^{-1} peak difference. The peak that was identified as the OH stretch of water is marked with an arrow (3610 cm^{-1} in $H_2{}^{16}O$, 2673 cm^{-1} in $D_2{}^{16}O$, and 3600 cm^{-1} in $H_2{}^{18}O$ spectra).

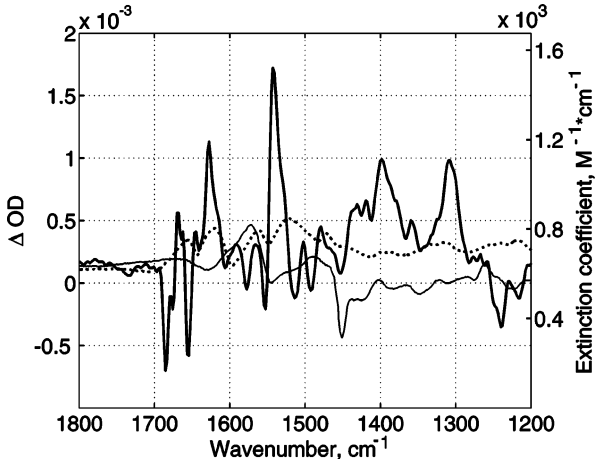

FIGURE 6: Comparison of extinction coefficients of the imidazole-minus-imidazolate His transition and the protonated-minus-deprotonated Lys transition together with acidic-minus-alkaline red-minus-ox FTIR spectra. The acidic-minus-alkaline (pH 5.2-minus-pH 9.5) red-minus-ox FTIR spectrum (thick solid line) is the same as in Figure 3 (solid line). The L-histidine (monomer), imidazole-minus-imidazolate spectrum (thin solid line) and the lysine (polymer), protonated-minus-deprotonated spectrum (dashed line) are normalized to the concentration of C*c*O. The spectra of histidine and lysine are reproduced from ref *22* and *43*, respectively. The spectrum of His was multiplied by a factor of 2 to get the extinction of the full imidazole/imidazolate transition. The extinction of the lysine transition is from ref *44*.

significantly higher than 10 (the 1740 cm^{-1} region is not significantly changed even at pH 10; our unpublished data) and even higher for the reduced enzyme. It may be noted that such a high pK_a for a carboxylic acid in a hydrophobic protein structure is not unprecedented as the value for aspartate 96 in bacteriorhodopsin, serving a similar function as glutamic acid 278 (*41*), has been estimated to be >11 (*42*).

The pH dependence of the acidic-minus-alkaline red-minus-ox FTIR spectra shows two transitions with apparent pK_a values of 6.6 and 8.4 and Hill coefficients of 0.9 and 0.1, respectively (Figure 4). The key question is, therefore, to what category (i−iii; see above) should these IR changes be ascribed?

The transition with pK_a 6.6 gives a Hill coefficient close to unity, which could therefore correspond to proton uptake/release by a single group or by several groups having very close pK_a values. However, neither transition shows any clear signature of a protolytic amino acid although contributions from protolytic amino acids with weak extinction coefficients of protonation are possible, e.g., the imidazolate → imidazole transition of His and the protonation of Lys. The protonation transitions of other protolytic amino acids have very prominent features with strong absorption (*43*, *44*) and should be recognized in the spectra if present. As an example, the double-difference spectrum is plotted in Figure 6 together with L-histidine imidazole-minus-imidazolate and protonated-minus-deprotonated lysine spectra, normalized to the C*c*O concentration. The concentration of rewetted enzyme on the ATR prism was estimated on the basis of the peptide bond extinction in the amide II band:

$$[\mathrm{C}c\mathrm{O}] = D/[\epsilon l N(k-4)]$$

where D is the optical density of amide II, ϵ is the extinction coefficient for a single peptide bond in the amide II band (M^{-1} cm^{-1}), 173 (*50*), l is the penetration depth (cm),

assumed as ~2 μm in the mid-infrared range based on extinction of H_2O (*45*), *N* is the number of bounces of the internal reflection element of the ATR prism, and *k* is the number of amino acid residues in the enzyme. This calculation yields an enzyme concentration [C*c*O] of ~3 mM.

Although our data cannot exclude protonation of metal-bound histidine or lysine, the pH effect on the double-difference FTIR spectra can hardly be assigned directly to protolytic reactions of amino acids but rather seems to reflect motions of the protein backbone and changes in hemes that are induced by protonation of, most likely, a number of groups with fractional protonation (case iii above). About one-half of the infrared features in the acidic-minus-alkaline red-minus-ox FTIR spectra exhibited two pH transitions. Therefore, these should be groups that feel both transitions and can be the hemes that are not protonated themselves but may sense these protolytic sites. The majority of the features in the double-difference spectra are intense (up to 2×10^3 M^{-1} cm^{-1} for the shift 1553/1543 cm^{-1}) and look like shifts rather than peaks or troughs. Heme absorption in the IR is much stronger than absorbance of amino acids, so that a small perturbation of the heme surroundings could cause a high contribution into these difference spectra.

H/D and $^{16}O/^{18}O$ Isotopic Exchange in the Water Region. The appearance of a "free" OH band from water was detected in the "water infrared region" on reduction of cytochrome oxidase. The peak at 3610 cm^{-1} in H_2O medium appeared to shift to 2673 cm^{-1} in D_2O medium and to 3600 cm^{-1} in $H_2{}^{18}O$. The H/D and $^{16}O/^{18}O$ shifts are about 940 and 10 cm^{-1}, respectively, which is in agreement with a shift of the hydroxyl stretching vibration in heavy water and $H_2{}^{18}O$ compared to H_2O (*45*). A similar band with H/D and $^{16}O/^{18}O$ shifts in the "water" region was earlier found for the water-oxidizing complex of photosystem II by Noguchi et al. (*46*) and assigned to water cleavage during the catalytic S-cycle. The position of the band observed here corresponds to a weakly H-bonded or free O−H vibration of water (*47*). This molecule must be asymmetric and the other O−H group may be strongly hydrogen-bonded with a corresponding vibrational mode at <3500 cm^{-1} with broad shape and weak extinction, which would be difficult to distinguish among the number of other bands.

Applying the extinction coefficient of the OH band of water estimated from experiments in ref *46* to our enzyme concentration and optical path length suggests that the band represents an OH vibration of a single water molecule per C*c*O molecule. This OH group may belong to a water molecule that is formed on enzyme reduction in the binuclear center, where metal-bound hydroxide may serve as an acceptor of a chemical proton. Alternatively, the band may derive from an internal water molecule, one OH group of which loses a hydrogen bond upon enzyme reduction.

Another prominent band at 3566 cm^{-1} that is sensitive to H/D but insensitive to $^{16}O/^{18}O$ water exchange, and to N^{14}/N^{15} global labeling (P. Rich, personal communication), belongs to a non-water O−H group, that becomes free on enzyme reduction. This band may originate, for example, from E-278 whose change of surroundings is seen around 1740 cm^{-1} (*34*). The band at 3566 cm^{-1} is shifted after H/D exchange to, probably, 2639 cm^{-1}.

There is also a weak band at 3672 cm^{-1} in H_2O medium and a band at 3558 cm^{-1} in both H_2O and D_2O. The first may belong to a free N−H group and the second to not exchangeable deeply buried free N−H. Four new features (2716, 2548, 2515, and 2473 cm^{-1}) that appear in D_2O probably belong to N−D stretching vibrations.

We conclude that the band at 3610 cm^{-1} may belong to a single asymmetric water molecule within the enzyme structure that could have been produced upon reduction of the binuclear center. The presence of an OH^- ligand at the Cu_B center was found in ref *48*, and a ferric heme a_3-OH state has been identified by Raman spectroscopy (*49*) in the oxidized state. It is possible that the water molecule is still weakly bound to one of these metal ions in the reduced state.

We have presented an attempt to discover the acceptors of protons taken up on reduction of cytochrome *c* oxidase. The IR water region shows the appearance of a vibration that is due to the OH stretch of structured asymmetric water. From this we conclude that at least one proton acceptor site for chemical protons may be OH^- in the binuclear center. If this is the case, the pK_a for such a water molecule should be at least 10 because of the absence of a pH dependence between pH 6.5 and pH 9.0. However, the found OH band may alternatively belong to a structured water molecule that loses one hydrogen bond upon reduction of the enzyme.

ACKNOWLEDGMENT

We are grateful to Eija Haasanen for enzyme purification, Dr. Kai Vuorilehto for the flow-through electrochemical cell, and Dr. Dmitry Bloch for help with data analysis. We thank Prof. Peter Rich for the microvolume electrochemical cell and for sharing unpublished data with us.

REFERENCES

1. Babcock, G. T., and Wikström, M. (1992) Oxygen activation and the conservation of energy in cell respiration, *Nature 356*, 301−309.
2. Michel, H., Behr, J., Harrenga, A., and Kannt, A. (1998) Cytochrome *c* oxidase: structure and spectroscopy, *Annu. Rev. Biophys. Biomol. Struct. 27*, 329−356.
3. Wikström, M. (2004) Cytochrome *c* oxidase: 25 years of the elusive proton pump, *Biochim. Biophys. Acta 1655*, 241−247.
4. Bloch, D., Belevich, I., Jasaitis, A., Ribacka, C., Puustinen, A., Verkhovsky, M. I., and Wikström, M. (2004) The catalytic cycle of cytochrome *c* oxidase is not the sum of its two halves, *Proc. Natl. Acad. Sci. U.S.A. 101*, 529−533.
5. Belevich, I., Verkhovsky, M. I., and Wikström, M. (2006) Proton-coupled electron transfer drives the proton pump of cytochrome *c* oxidase, *Nature 440*, 829−832.
6. Brändén, G., Gennis, R. B., and Brzezinski, P. (2006) Transmembrane proton translocation by cytochrome *c* oxidase, *Biochim. Biophys. Acta 1757*, 1052−1063.
7. Oliveberg, M., Brzezinski, P., and Malmström, B. G. (1989) The effect of pH and temperature on the reaction of fully reduced and mixed-valence cytochrome *c* oxidase with dioxygen, *Biochim. Biophys. Acta 977*, 322−328.
8. Zaslavsky, D., Kaulen, A., Smirnova, I. A., Vygodina, T. V., and Konstantinov, A. A. (1993) Flash-induced membrane potential generation by cytochrome *c* oxidase, *FEBS Lett. 336*, 389−393.
9. Siletsky, S. A., Kaulen, A. D., Mitchell, D., Gennis, R. B., and Konstantinov, A. A. (1996) Resolution of two proton conduction pathways in cytochrome *c* oxidase, *EBEC Short Rep. 9*, 90.
10. Verkhovsky, M. I., Belevich, I., Bloch, D. A., and Wikström, M. (2006) Elementary steps of proton translocation in the catalytic cycle of cytochrome oxidase, *Biochim. Biophys. Acta 1757*, 401−407.
11. Iwata, S., Ostermeier, C., Ludwig, B., and Michel, H. (1995) Structure at 2.8 Å resolution of cytochrome *c* oxidase from *Paracoccus denitrificans*, *Nature 376*, 660−669.
12. Tsukihara, T., Aoyama, H., Yamashita, E., Takashi, T., Yamaguchi, H., Shinzawa-Itoh, K., Nakashima, R., Yaono, R., and

Yoshikawa, S. (1996) The whole structure of the 13-subunit oxidized cytochrome *c* oxidase at 2.8 Å, *Science 272*, 1136−1144.
13. Svensson, E., Abramson, J., Larsson, G., Tornroth, S., Brzezinski, P., and Iwata, S. (2002) The X-ray crystal structures of wild-type and EQ(I-286) mutant cytochrome *c* oxidases from *Rhodobacter sphaeroides*, *J. Mol. Biol. 321*, 329−339.
14. Qin, L., Hiser, C., Mulichak, A., Garavito, R. M., and Ferguson-Miller, S. (2006) Identification of conserved lipid/detergent-binding sites in a high-resolution structure of the membrane protein cytochrome c oxidase, *Proc. Natl. Acad. Sci. U.S.A. 103*, 16117−16122.
15. Tsukihara, T., Shimokata, K., Katayama, Y., Shimada, H., Muramoto, K., Aoyama, H., Mochizuki, M., Shinzawa-Itoh, K., Yamashita, E., Yao, M., Ishimura, Y., and Yoshikawa, S. (2003) The low-spin heme of cytochrome *c* oxidase as the driving element of the proton-pumping process, *Proc. Natl. Acad. Sci. U.S.A. 100*, 15304−15309.
16. Braiman, M. S., and Rothschild, K. J. (1988) Fourier transform infrared techniques for probing membrane protein structure, *Annu. Rev. Biophys. Biophys. Chem. 17*, 541−570.
17. Heberle, J. (2000) Proton transfer reactions across bacteriorhodopsin and along the membrane, *Biochim. Biophys. Acta 1458*, 135−147.
18. Garczarek, F., and Gerwert, K. (2006) Functional waters in intraprotein proton transfer monitored by FTIR difference spectroscopy, *Nature 439*, 109−112.
19. Heberle, J., and Zscherp, C. (1996) ATR/FT-IR difference spectroscopy of biological matter with microsecond time resolution, *Appl. Spectrosc. 50*, 588−596.
20. Scheirlinckx, F., Buchet, R., Ruysschaert, J. M., and Goormaghtigh, E. (2001) Monitoring of secondary and tertiary structure changes in the gastric H^+/K^+-ATPase by infrared spectroscopy, *Eur. J. Biochem. 268*, 3644−3653.
21. Rich, P. R., and Breton, J. (2002) Attenuated total reflection Fourier transform infrared studies of redox changes in bovine cytochrome *c* oxidase: resolution of the redox Fourier transform infrared difference spectrum of heme a_3, *Biochemistry 41*, 967−973.
22. Iwaki, M., Yakovlev, G., Hirst, J., Osyczka, A., Dutton, P. L., Marshall, D., and Rich, P. R. (2005) Direct observation of redox-linked histidine protonation changes in the iron-sulfur protein of the cytochrome bc_1 complex by ATR-FTIR spectroscopy, *Biochemistry 44*, 4230−4237.
23. Iwaki, M., Andrianambinintsoa, S., Rich, P., and Breton, J. (2002) Attenuated total reflection Fourier transform infrared spectroscopy of redox transitions in photosynthetic reaction centers: comparison of perfusion- and light-induced difference spectra, *Spectrochim. Acta, Part A 58*, 1523−1533.
24. Iwaki, M., Puustinen, A., Wikström, M., and Rich, P. R. (2003) ATR-FTIR spectroscopy of the P(M) and F intermediates of bovine and *Paracoccus denitrificans* cytochrome *c* oxidase, *Biochemistry 42*, 8809−8817.
25. Iwaki, M., Puustinen, A., Wikström, M., and Rich, P. R. (2006) Structural and chemical changes of the P(M) intermediate of *Paracoccus denitrificans* cytochrome *c* oxidase revealed by IR spectroscopy with labeled tyrosines and histidine, *Biochemistry 45*, 10873−10885.
26. Hellwig, P., Behr, J., Ostermeier, C., Richter, O. M. H., Pfitzner, U., Odenwald, A., Ludwig, B., Michel, H., and Mäntele, W. (1998) Involvement of glutamic acid 278 in the redox reaction of the cytochrome *c* oxidase from *Paracoccus denitrificans* investigated by FTIR spectroscopy, *Biochemistry 37*, 7390−7399.
27. Hellwig, P., Pfitzner, U., Behr, J., Rost, B., Pesavento, R. P., Donk, W. V., Gennis, R. B., Michel, H., Ludwig, B., and Mäntele, W. (2002) Vibrational modes of tyrosines in cytochrome *c* oxidase from *Paracoccus denitrificans*: FTIR and electrochemical studies on Tyr-D4-labeled and on Tyr280His and Tyr35Phe mutant enzymes, *Biochemistry 41*, 9116−9125.
28. Iwaki, M., Puustinen, A., Wikström, M., and Rich, P. R. (2004) ATR-FTIR spectroscopy and isotope labeling of the PM intermediate of *Paracoccus denitrificans* cytochrome *c* oxidase, *Biochemistry 43*, 14370−14378.
29. Gorbikova, E. A., Vuorilehto, K., Wikström, M., and Verkhovsky, M. I. (2006) Redox titration of all electron carriers of cytochrome *c* oxidase by fourier transform infrared spectroscopy, *Biochemistry 45*, 5641−5649.
30. Mitchell, R., and Rich, P. R. (1994) Proton uptake by cytochrome *c* oxidase on reduction and on ligand binding, *Biochim. Biophys. Acta 1186*, 19−26.
31. Ribacka, C., Verkhovsky, M. I., Belevich, I., Bloch, D. A., Puustinen, A., and Wikström, M. (2005) An elementary reaction step of the proton pump is revealed by mutation of tryptophan-164 to phenylalanine in cytochrome *c* oxidase from *Paracoccus denitrificans*, *Biochemistry 44*, 16502−16512.
32. Vuorilehto, K., Lütz, S., and Wandrey, C. (2004) Indirect electrochemical reduction of nicotinamide coenzymes, *Bioelectrochemistry 65*, 1−7.
33. Rath, P., Degrip, W. J., and Rothschild, K. J. (1998) Photoactivation of rhodopsin causes an increased hydrogen-deuterium exchange of buried peptide groups, *Biophys. J. 74*, 192−198.
34. Verkhovskaya, M. L., Garcia-Horsman, A., Puustinen, A., Rigaud, J. L., Morgan, J. E., Verkhovsky, M. I., and Wikström, M. (1997) Glutamic acid 286 in subunit I of cytochrome bo_3 is Involved in proton translocation, *Proc. Natl. Acad. Sci. U.S.A. 94*, 10128−10131.
35. Lübben, M., Prutsch, A., Mamat, B., and Gerwert, K. (1999) Electron transfer induces side-chain conformational changes of glutamate-286 from cytochrome bo_3, *Biochemistry 38*, 2048−2056.
36. Mitchell, R., and Rich, P. R. (1994) Proton uptake by cytochrome *c* oxidase on reduction and on ligand binding, *Biochim. Biophys. Acta 1186*, 19−26.
37. Capitanio, N., Capitanio, G., De, Nitto, E., Boffoli, D., and Papa, S. (2003) Proton transfer reactions associated with the reaction of the fully reduced, purified cytochrome *c* oxidase with molecular oxygen and ferricyanide, *Biochemistry 42*, 4607−4612.
38. Smirnova, I., Ädelroth, P., Gennis, R. B., and Brzezinski, P. (1999) Aspartate-132 in cytochrome *c* oxidase from *Rhodobacter sphaeroides* is involved in a two-step proton transfer during oxo-ferryl formation, *Biochemistry 38*, 6826−6833.
39. Karpefors, M., Ädelroth, P., Zhen, Y., Ferguson-Miller, S., and Brzezinski, P. (1998) Proton uptake controls electron transfer in cytochrome *c* oxidase, *Proc. Natl. Acad. Sci. U.S.A. 95*, 13606−13611.
40. Namslauer, A., Aagaard, A., Katsonouri, A., and Brzezinski, P. (2003) Intramolecular proton-transfer reactions in a membrane-bound proton pump: the effect of pH on the peroxy to ferryl transition in cytochrome *c* oxidase, *Biochemistry 42*, 1488−1498.
41. Wikström, M., Morgan, J. E., and Verkhovsky, M. (1998) On the mechanism of proton translocation by respiratory enzyme, *J. Bioenerg. Biomembr. 30*, 139−145.
42. Szaraz, S., Oesterhelt, D., and Ormos, P. (1994) pH-induced structural changes in bacteriorhodopsin studied by Fourier transform infrared spectroscopy, *Biophys. J. 67*, 1706−1712.
43. Rich, P. R., and Iwaki, M. (2005) Infrared protein spectroscopy as a tool to study protonation reactions within proteins, in *Biophysical and Structural Aspects of Bioenergetics* (Wikström, M., Ed.) pp 314−333, RSC Publishing, Cambridge, U.K.
44. Barth, A. (2000) The infrared absorption of amino acid side chains, *Prog. Biophys. Mol. Biol. 74*, 141−173.
45. Lappi, S. E., Smith, B., and Franzen, S. (2004) Infrared spectra of $H_2{}^{16}O$, $H_2{}^{18}O$ and D_2O in the liquid phase by single-pass attenuated total internal reflection spectroscopy, *Spectrochim. Acta, Part A 60*, 2611−2619.
46. Noguchi, T., and Sugiura, M. (2002) FTIR detection of water reactions during the flash-induced S-state cycle of the photosynthetic water-oxidizing complex, *Biochemistry 41*, 15706−15712.
47. Szymanski, H. A. (1967) *Interpreted Infrared Spectra*, Plenum Press, New York.
48. Fann, Y. C., Ahmed, I., Blackburn, N. J., Boswell, J. S., Verkhovskaya, M. L., Hoffman, B. M., and Wikström, M. (1995) Structure of Cu_B in the binuclear heme-copper center of the cytochrome aa_3-type quinol oxidase from *Bacillus subtilis*: An ENDOR and EXAFS study, *Biochemistry 34*, 10245−10255.
49. Han, S., Ching, Y. C., and Rousseau, D. L. (1990) Ferryl and hydroxy intermediates in the reaction of oxygen with reduced cytochrome *c* oxidase, *Nature 348*, 89−90.
50. Rahmelow, K., Hübner, W., and Ackermann, T. (1998) Infrared absorbances of protein side chains, *Anal. Biochem. 257*, 1−11.

BI602523A